Selective Fluorescence Detection of Monosaccharides Using a Material Composite Formed between Graphene Oxide and Boronate-Based Receptors

Xiaolong Sun,[†,‡] Bin Zhu,[§,‡] Ding-Kun Ji,[§] Qibin Chen,[§] Xiao-Peng He,*[,§] Guo-Rong Chen,[§] and Tony D. James*[,†]

[§]Key Laboratory for Advanced Materials & Institute of Fine Chemicals, East China University of Science and Technology, Shanghai 200237, P.R. China

[†]Department of Chemistry, University of Bath, Bath, BA2 7AY, U.K.

S *Supporting Information*

ABSTRACT: We have developed a novel class of simple materials for sensing monosaccharides by the functionalization of graphene oxide (GO) with boronate-based fluorescence probes (**BA1** and **BA2**). The composite materials were characterized by atomic force microscopy, Raman spectroscopy, and UV−vis/fluorescence spectroscopy. The strong fluorescence of the **BA** probes is quenched in the presence of GO through fluorescence resonance energy transfer. The **BA**@GO composite sensors formed provide a useful platform for *fluorogenic* detection of monosaccharides based on the strong affinity between the boronic acid receptor and monosaccharides. The **BA**@GO composite sensor displayed a "turn-on" fluorescence response with a good linear relationship toward fructose over a range of other saccharides.

KEYWORDS: *graphene oxide, boronic acid, monosaccharide, fluorescence sensing, nanocomposite, fructose*
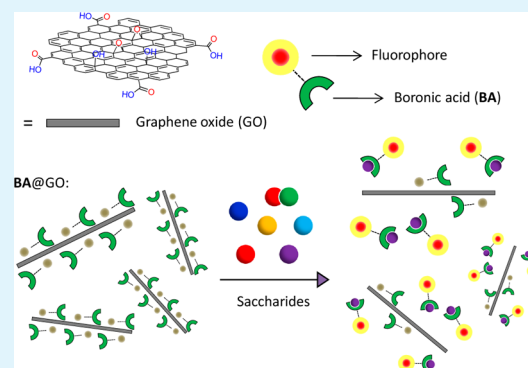
INTRODUCTION

Boronic acids have been exploited extensively as chemo/biosensors in the detection of saccharides, anion, and reactive oxygen species/reactive nitrogen species through electrochemical, fluorescence (FL), and colorimetric measurements.[1−3] Notably, boronic acids are excellent molecular receptors for monosaccharide because boronic acid (BA) derivatives rapidly and reversibly interact with saccharides in aqueous media, and thus, importantly, the method does not consume the analyte. The chemical and biological significance of the interaction between BA and saccharides has been extensively used for the study of saccharide detection via FL methods.[1,4]

However, limited work has been carried out in the development of FL materials for chemical sensing of sugars via BA−saccharide interaction.[5−7] Among them, Strano et al. developed a series of BA constructs to sodium cholate-suspended single-wall nanotubes (SC/SWNTs) and have screened the resulting complexes for their ability to modulate FL emission response to glucose. However, the selectivity and sensitivity of BA−SWNT complexes toward saccharides were suboptimal and thus hampered their further application.[8]

Graphene oxide (GO), because of its good optical and electrical properties, good water solubility, and low toxicity to the human body, has become a promising material of choice in the development of chemo- and biosensors.[9,10] In particular,

GO has been shown to be a universal quencher of nearly all fluorescent dyes by taking advantage of the fluorescence resonance energy-transfer (FRET) mechanism.[11,12] As a result, GO-based fluorogenic (fluorescence "off−on") sensors that embody a fluorophore functionalized with biomolecules stacked to GO for detection of DNA, proteins, enzymes, microbes, and live cancer cells have been devised.[13−20,27]

These GO composites are advantageous in that they are economic and simple to prepare, and a recent study reveals that the two-dimensional GO material is a better choice in DNA analysis than either SWNT (one-dimensional) or gold nanoparticles (zero-dimensional).[21] Therefore, we hypothesized that the complexation of monosaccharides with an aromatic BA probe conjugated on the surface of GO, presumably through stacking between the graphene plane and aromatic moiety of FL probes, could modulate the FL signal in response to the binding of saccharides (Figure 1). We found that FL of the **BA**@GO complex, quenched by the attachment of simple mono-BA fluorophore to GO, can be recovered in response to binding of fructose, among the saccharides. We believe that the simplicity of our method coupled with the possibility for extension toward a general sensing platform for
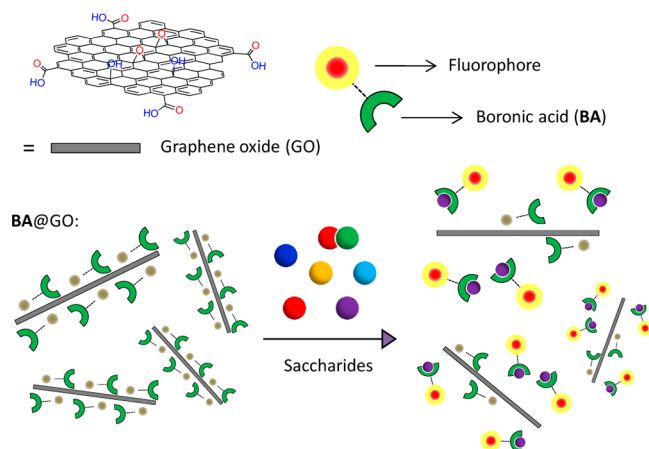
Figure 1. Schematic representation of the designed fluorogenic **BA**@GO sensors for the selective detection of monosaccharides.

other saccharides can provide new insight into developing advanced fluorogenic materials.

RESULTS AND DISCUSSION

Probe **BA1** (λ_{abs} = 440 nm and ϵ = 9500 M^{-1}cm^{-1}; Scheme 1) was designed based on the photoinduced electron-transfer

Scheme 1. Synthetic Route for BA1 and BA2
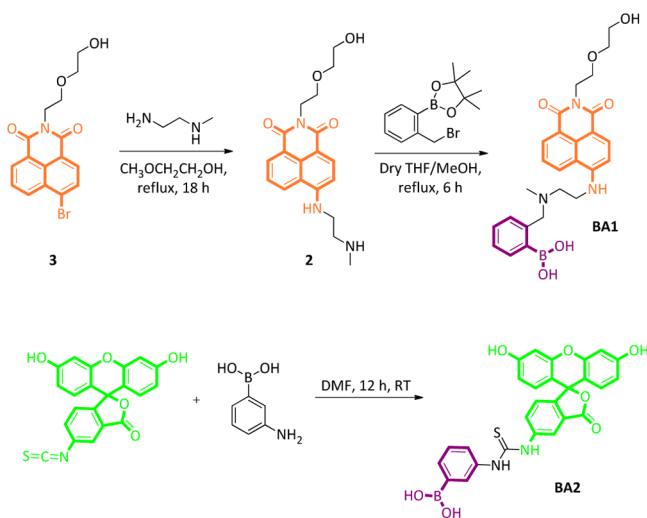
mechanism.[22] N-Substituted 1,8-naphthalimide is an excellent D−π−A chromophore with good photophysical and photochemical properties. The system displays an "off−on" response toward monosaccharides due to enhanced N−B interaction.[23] Probe **BA2** (λ_{abs} = 490 nm and ϵ = 91900 M^{-1}cm^{-1}; Scheme 1) was synthesized by incorporating (3-aminophenyl)boronic acid with fluorescein isothiocyanate in *N,N*-dimethylformamide.[24] In addition, fluorescein has been widely used in biological research and health care because of its good biocompability, bioorthogonality, and nontoxicity. In both cases, the BA moiety is recognized as an excellent binding motif for saccharides, even when functionalized at an interface.[25,26]

The **BA1**@GO and **BA2**@GO composites were formed by mixing boronic acids (**BA1** and **BA2**) with fresh-made GO in situ.[20] The **BA1**@GO composite material was chosen as a model to be characterized by various techniques. Atomic force microscopy (AFM) was used to measure the height of the GO

flakes. Whereas the height of unmodified GO measures 1.2 nm (Figure 2a), that of GO stacked with **BA1** grows to 1.8 nm; the
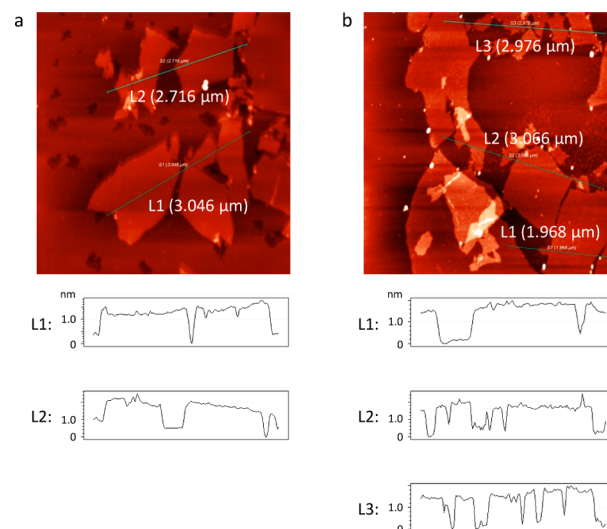

Figure 2. AFM images of (a) GO and (b) **BA1**@GO.

latter indicates composite formation of GO with **BA1**. Note that all intersected surface areas of **BA1**@GO showed a similar height increase of about 0.6 nm, indicating that the compound was densely distributed on the surface.

Raman spectroscopy additionally corroborated the composition of the composite (Figure S1a in the Supporting Information, SI): the ratio of the intensity of the D band (1355 cm^{-1}) to that of the G band (1600 cm^{-1}) of **BA1**@GO (0.91) is greater than that bare GO (0.86), which means that the C sp^2 hybridization of the former is increased upon stacking with the aromatic compound.[11,12] Meanwhile, through stacking with **BA1**, a new peak characteristic of GO appeared at 450 nm in the UV−vis spectrum (Figure S1b in the SI), which also manifests formation of the **BA1**@GO composite.

In the case of **BA1**, the presence of 40 μg/mL of GO led to almost complete FL quenching of the probe $[(F_0 − F)/F_0 = 97.4\%$, where F is the FL of **BA1** with GO and F_0 that without GO] (Figure 3a). A good linear response in the presence of increasing GO (0−12 μg/mL) was observed (R^2 = 0.9955; Figure 3b). The quenching is probably due to the fact that, when the FL probes are stacked to GO, the photoexcited energy is transferred from the naphthalimide fluorophore to the GO acceptor.[11,12]

Subsequently, in the presence of increasing fructose (0−2 M), the maximum FL of **BA1** at 525 nm was gradually recovered with a maximum recovery ratio $[(F_1 − F)/(F_0 − F)$, where F is the FL of **BA1** with GO, F_0 that without GO, and F_1 that of **BA1**@GO with fructose] of 32.2% (Figure 3c; the linear range of FL recovery is shown in Figure 3d; R^2 = 0.9925). The detection limit of **BA1**@GO for fructose was determined to be 2.7 mM ($3\sigma/k$). Meanwhile, we determined that, for the free **BA1** probe, the addition of fructose (0−1 M) led to a 2.8-fold FL increase of the probe (2 μM) due to enhanced N−B interaction in aqueous solution (pH 9.0; Figure S3 in the SI). We ascribe the "turn-on" response of the **BA1**@GO composite to the specific covalent bonding of the BA of **BA1** with fructose, leading to an increase in the hydrophilicity of the resulting **BA1**−saccharide complex, which causes the complex to detach from the GO surface (i.e., weakened π stacking). The release of
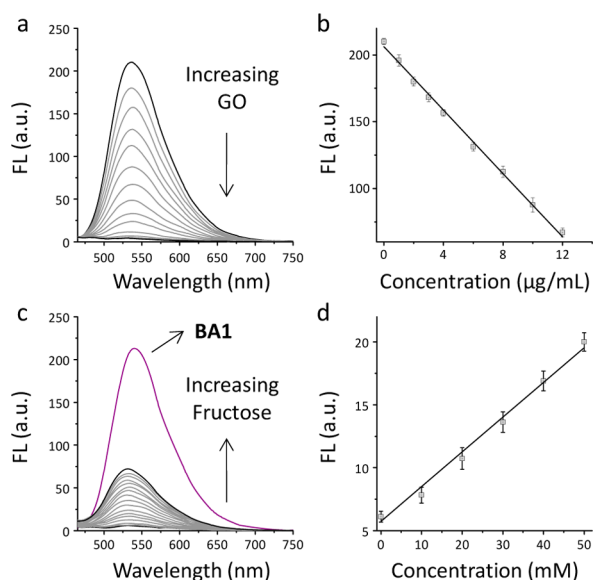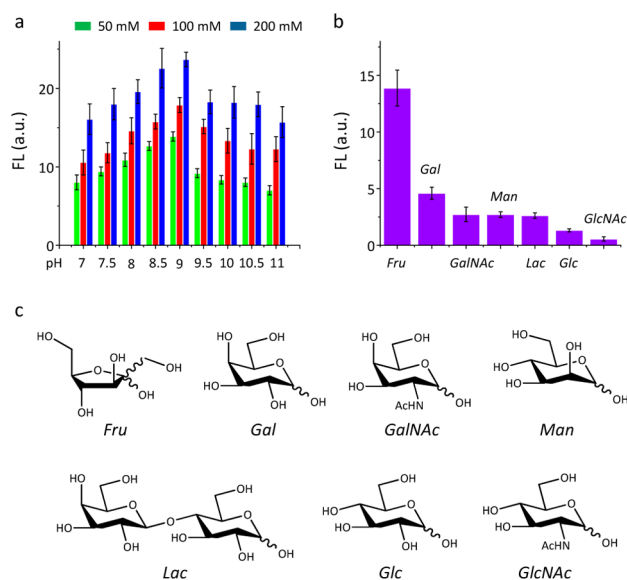
Figure 3. (a) FL change of **BA1** (2 μM) in the presence of increasing GO (0−45 μg/mL) in Tris-HCl (0.05 M, pH 7.3). (b) Linear range of FL change of **BA1** at 525 nm in the presence of increasing GO (0−12 μg/mL). (c) FL change of **BA1@GO** (2 μM) in the presence of increasing fructose (0−2 M; the violet curve is the FL spectrum of **BA1**) in Tris-HCl (0.05 M, pH 9.0). (d) Linear range of FL change of **BA1** at 525 nm in the presence of increasing fructose (λ_{ex} = 410 nm).

Figure 4. (a) FL change of **BA1@GO** in the presence of fructose in 0.05 M Tris-HCl with different pH values. (b) FL change of **BA1@GO** in the presence of 50 mM of different saccharides (where Fru is fructose, Gal is galactose, GalNAc is *N*-acetylgalactosamine, Man is mannose, Lac is lactose, Glc is glucose, and GlcNAc is *N*-acetylglucosamine) in Tris-HCl (0.05 M, pH 9.0; λ_{ex} = 410 nm). (c) Structures of the various monosaccharides.

the complex from the surface then leads to the recovery of FL of the probe because the surface quenching by FRET to the GO surface is now not possible. However, the incomplete FL recovery indicates that part of the small-molecule probe was still linked with GO likely because of strong stacking forces.

In contrast, while the maximum FL intensity of **BA2** could be similarly quenched adequately in the presence of 40 μg/mL of GO [$(F_0 − F)/F_0$ = 97.4%; Figure S2 in the SI], compared with **BA1**, the presence of excessive fructose (2 M) barely induced its FL recovery (recovery rate = 2.7%; Figure S2 in the SI). For the free **BA2** probe, the addition of fructose (0−1 M) led to a slight FL decrease of the probe **BA2** (0.5 μM) in an aqueous solution (pH 9.0; Figure S2 in the SI). As a result, the minimum FL recovery of **BA2** toward fructose could be due to a stronger interaction of the more rigid fluorophore receptor system of **BA2** with the GO surface (**BA1** has a more flexible linkage between the fluorophore and BA receptor). However, it could also be due to the inherent quenching and low sensitivity of the **BA2** system toward fructose (Figure S3 in the SI). Consequently, **BA1** was selected for further detailed analyses.

By varying the pH from 7 to 11, we determined that the sensitivity of **BA1@GO** increased to a maximum at pH 9 but weakened with a further increase of the pH (Figures 4a, Figure S4 in the SI). The selectivity of **BA1@GO** was investigated with a range of different saccharides that are important cell-membrane components of mamanlian cells. As shown in Figure 4b, in the presence of 50 mM of different saccharides including fructose, galactose, *N*-acetylgalactosamine, mannose, lactose, glucose, and *N*-acetylglucosamine, the sensor only showed a significant fluorogenic response to fructose (Figure S5 in the SI). This is the expected selectivity for a simple mono-BA-based system.[4] Our approach suggests that saccharide-selective optical off−on sensors can be developed based on the stacking of fluorescent boronic acids to GO, since in order to develop **BA@GO** systems with appropriate saccharide selectivity,

composite materials constructed using BA-based receptors with the required saccharide selectivity must be prepared.

CONCLUSION

In summary, we have developed a **BA@GO** composite material for the detection of saccharides. Upon the stacking of a fluorescent **BA** onto the surface of GO, a quenched optical material was fabricated. The sensor was found to be selective for fructose among a panel of biologically important saccharides, producing a fluorogenic signal response. This study sets the basis for the development of a new generation of boronate-based saccharide sensors, using simple and economic GO composite materials. We believe that this model **BA@GO** composite sensor represents a promising sensing strategy for the detection of biologically important sugars. The fabrication of **BA@GO** systems with improved sensitivity and selectivity is currently underway in our laboratories.

EXPERIMENTAL SECTION

Synthesis of Compound 3. Under a nitrogen atmosphere, to a solution of 4-bromo-1,8-naphthalic anhydride (0.30 g, 1.08 mmol) in anhydrous ethanol (20 mL) was added 2-(2-aminoethoxy)ethanol (0.12 g, 1.19 mmol). The mixture was heated at reflux for 3 h and concentrated under reduced pressure. Purification by flash chromatography [50:1 (v/v) CH$_2$Cl$_2$/CH$_3$OH] afforded a yellow powder (0.35 g). Yield: 88%. Mp: 122−124 °C. ^{1}H NMR (300 MHz, CDCl$_3$): δ 8.60 (d, J = 7.5 Hz, 1H), 8.53 (d, J = 8.4 Hz, 1H), 8.36 (d, J = 7.8 Hz, 1H), 7.98 (d, J = 7.8 Hz, 1H), 7.79 (dd, J_1 = 8.4 Hz, J_2 = 7.2 Hz, 1H), 4.38 (t, $J_1 = J_2$ = 5.4 Hz, 2H), 3.79 (t, $J_1 = J_2$ = 5.7 Hz, 2H), 3.59−3.63 (m, 4H). ^{13}C NMR (75 MHz, CDCl$_3$): δ 163.9, 163.8, 133.4, 132.2, 131.4, 131.1, 130.5, 128.9, 128.1, 122.8, 121.9, 72.3, 68.3, 61.8, 39.6. HRMS (ESI$^+$). Calcd for [M + Na]$^+$: m/z 386.0004. Found: m/z 386.0028.

Synthesis of Compound 2. A solution of (2-bromoethyl)amine hydrobromide (1.5 g, 4.12 mmol) and *N*-methylethylenediamine (0.322 g, 95 wt %, 4.12 mmol) in 2-methoxyethanol was refluxed overnight under a nitrogen atmosphere. The mixture was concentrated

10080

dx.doi.org/10.1021/am500801g | *ACS Appl. Mater. Interfaces* 2014, 6, 10078−10082

under reduced pressure to obtain a purple oil product. Column chromatography on silica gel [3:1 (v/v) CH_2Cl_2/CH_3OH] was employed to purify the crude product as red oil (0.8 g). Yield: 55%. ^1H NMR (300 MHz, $CDCl_3$): δ 8.49 (dd, J_1 = 7.5 Hz, J_2 = 0.9 Hz 1H), 8.39 (d, J = 8.4 Hz, 1H), 8.19 (dd, J_1 = 8.7 Hz, J_2 = 0.9 Hz 1H), 7.55 (dd, J_1 = 8.4 Hz, J_2 = 7.5 Hz, 1H), 6.59 (d, J = 8.4 Hz, 1H), 6.39 (br s, 1H), 4.41 (t, J_1 = J_2 = 5.4 Hz, 2H), 3.87 (t, J_1 = J_2 = 5.4 Hz, 2H), 3.72 (m, 4H), 3.48 (m, 2H), 3.07 (t, J_1 = J_2 = 6.0 Hz, 2H), 2.54 (s, 3H). ^{13}C NMR (75 MHz, $CDCl_3$): δ 165.0, 164.5, 150.0, 134.6, 131.2, 129.6, 126.9, 124.4, 122.3, 120.2, 109.4, 104.1, 72.4, 68.8, 61.7, 50.8, 42.1, 39.3, 35.9. HRMS (ESI$^+$). Calcd for [M + H]$^+$: m/z 358.1766. Found: m/z 358.1772.

Synthesis of BA1. The product compound **BA1** was synthesized by refluxing compound **2** (0.20 g, 0.56 mmol) with (2-bromomethylphenyl)boronic acid pinacol ester (0.28 g, 0.94 mmol) in dry tetrahydrofuran (20 mL) for 6 h. The product was purified on silica gel, using 5:1 dichloromethane/methanol to afford **BA1** as a yellow solid (0.07 g). Yield: 25%. Mp: 119−121 °C. ^1H NMR (300 MHz, CD_3OD): δ 8.60 (d, J = 8.4 Hz, 1H), 8.44 (d, J = 7.2 Hz, 1H), 8.28 (d, J = 8.4 Hz, 1H), 7.58 (dd, J_1 = J_2 = 8.1 Hz, 2H), 7.22 (m, 3H), 6.80 (d, J = 8.4 Hz, 1H), 4.32 (t, J_1 = J_2 = 6.0 Hz, 2H), 4.17 (s, 2H), 3.74−3.84 (m, 4H), 3.57−3.63 (m, 4H), 3.29−3.34 (m, 2H), 2.59 (s, 3H). ^{13}C NMR (75 MHz, CD_3OD): δ 166.6, 166.1, 152.4, 136.2, 134.6, 132.6, 131.5, 130.3, 128.8, 128.6, 128.5, 125.9, 123.6, 122.4, 110.5, 105.5, 73.8, 69.6, 64.7, 62.6, 56.3, 41.7, 40.5, 39.8. HRMS (ESI$^+$). Calcd for [M + H]$^+$: m/z 492.2305. Found: m/z 492.2326.

AFM. A morphology study was performed with an atomic force microscope (AJ-III, Aijian Nanotechnology Inc., China) in air under tapping mode at room temperature. The samples used were dispersed on freshly cleaved mica and then dried at room temperature.

Raman Spectroscopy. Raman spectra were performed on a Renishaw InVia Reflex Raman system (Renishaw plc, Wotton-under-Edge, U.K.) by employing a grating spectrometer with a Peltier-cooled charge-coupled-device (CCD) detector coupled to a confocal microscope, which were then processed with Renishaw *WiRE 3.2* software. The Raman scattering was excited by an argon-ion laser (I = 514.5 nm).

FL Spectroscopy. All FL spectra of **BA1** were recorded with an excitation of 410 nm, while **BA2** were recorded with an excitation of 450 nm, and the emissions were scanned from 450 to 700 nm. Saccharides were incubated with **BA@GO** and **BA** in a Tris-HCl buffer (0.05 M, different pH values). The resulting mixture was incubated at room temperature for 5 min before the FL intensity was recorded.

ASSOCIATED CONTENT

ⓢ Supporting Information

Additional figures and NMR copies of new compounds. This material is available free of charge via the Internet at http://pubs.acs.org.

AUTHOR INFORMATION

Corresponding Authors
*E-mail: xphe@ecust.edu.cn.
*E-mail: t.d.james@bath.ac.uk.

Author Contributions
‡X.S. and B.Z. contributed equally.

Notes
The authors declare no competing financial interest.

ACKNOWLEDGMENTS

REFERENCES

(1) Wu, X.; Li, Z.; Chen, X. X.; Fossey, J. S.; James, T. D.; Jiang, Y. B. Selective sensing of saccharides using simple boronic acids and their aggregates. *Chem. Soc. Rev.* **2013**, *42*, 8032−8048.

(2) Xu, Z.; Kim, S. K.; Han, S. J.; Lee, C.; Kociok-Kohn, G.; James, T. D.; Yoon, J. Ratiometric Fluorescence Sensing of Fluoride Ions by an Asymmetric Bidentate Receptor Containing a Boronic Acid and Imidazolium Group. *Eur. J. Org. Chem.* **2009**, *2009*, 3058−3065.

(3) Lippert, A. R.; Van de Bittner, G. C.; Chang, C. J. Boronate Oxidation as a Bioorthogonal Reaction Approach for Studying the Chemistry of Hydrogen Peroxide in Living Systems. *Acc. Chem. Res.* **2011**, *44*, 793−804.

(4) Bull, S. D.; Davidson, M. G.; van den Elsen, J. M.; Fossey, J. S.; Jenkins, A. T.; Jiang, Y. B.; Kubo, Y.; Marken, F.; Sakurai, K.; Zhao, J.; James, T. D. Exploiting the reversible covalent bonding of boronic acids: recognition, sensing, and assembly. *Acc. Chem. Res.* **2013**, *46*, 312−326.

(5) Li, Y.-H.; Zhang, L.; Huang, J.; Liang, R.-P.; Qiu, J.-D. Fluorescent graphene quantum dots with a boronic acid appended bipyridinium salt to sense monosaccharides in aqueous solution. *Chem. Commun.* **2013**, *49*, 5180−5182.

(6) Qu, Z.-b.; Zhou, X.; Gu, L.; Lan, R.; Sun, D.; Yu, D.; Shi, G. Boronic acid functionalized graphene quantum dots as a fluorescent probe for selective and sensitive glucose determination in micro-dialysate. *Chem. Commun.* **2013**, *49*, 9830−9832.

(7) Mu, B.; McNicholas, T. P.; Zhang, J.; Hilmer, A. J.; Jin, Z.; Reuel, N. F.; Kim, J.-H.; Yum, K.; Strano, M. S. A Structure−Function Relationship for the Optical Modulation of Phenyl Boronic Acid-Grafted, Polyethylene Glycol-Wrapped Single-Walled Carbon Nanotubes. *J. Am. Chem. Soc.* **2012**, *134*, 17620−17627.

(8) Yum, K.; Ahn, J.-H.; McNicholas, T. P.; Barone, P. W.; Mu, B.; Kim, J.-H.; Jain, R. M.; Strano, M. S. Boronic Acid Library for Selective, Reversible Near-Infrared Fluorescence Quenching of Surfactant Suspended Single-Walled Carbon Nanotubes in Response to Glucose. *ACS Nano* **2011**, *6*, 819−830.

(9) Novoselov, K. S.; Geim, A. K.; Morozov, S. V.; Jiang, D.; Zhang, Y.; Dubonos, S. V.; Grigorieva, I. V.; Firsov, A. A. Electric Field Effect in Atomically Thin Carbon Films. *Science* **2004**, *306*, 666−669.

(10) Liao, K.-H.; Lin, Y.-S.; Macosko, C. W.; Haynes, C. L. Cytotoxicity of Graphene Oxide and Graphene in Human Erythrocytes and Skin Fibroblasts. *ACS Appl. Mater. Interfaces* **2011**, *3*, 2607−2615.

(11) Kim, J.; Cote, L. J.; Kim, F.; Huang, J. Visualizing Graphene Based Sheets by Fluorescence Quenching Microscopy. *J. Am. Chem. Soc.* **2010**, *132*, 260−267.

(12) Morales-Narváez, E.; Merkoçi, A. Graphene Oxide as an Optical Biosensing Platform. *Adv. Mater.* **2012**, *24*, 3298−3308.

(13) Geim, A. K.; Novoselov, K. S. The rise of graphene. *Nat. Mater.* **2007**, *6*, 183−191.

(14) Geim, A. K. Graphene: Status and Prospects. *Science* **2009**, *324*, 1530−1534.

(15) Jung, J. H.; Cheon, D. S.; Liu, F.; Lee, K. B.; Seo, T. S. A Graphene Oxide Based Immuno-biosensor for Pathogen Detection. *Angew. Chem., Int. Ed.* **2010**, *49*, 5708−5711.

(16) Wang, L.; Pu, K.-Y.; Li, J.; Qi, X.; Li, H.; Zhang, H.; Fan, C.; Liu, B. A Graphene-Conjugated Oligomer Hybrid Probe for Light-Up Sensing of Lectin and Escherichia Coli. *Adv. Mater.* **2011**, *23*, 4386−4391.

(17) Liu, Y.; Dong, X.; Chen, P. Biological and chemical sensors based on graphene materials. *Chem. Soc. Rev.* **2012**, *41*, 2283−2307.

(18) Feng, L.; Wu, L.; Qu, X. New Horizons for Diagnostics and Therapeutic Applications of Graphene and Graphene Oxide. *Adv. Mater.* **2013**, *25*, 168−186.

(19) Li, Z.; Deng, S. S.; Zang, Y.; Gu, Z.; He, X. P.; Chen, G. R.; Chen, K.; James, T. D.; Li, J.; Long, Y. T. Capturing intercellular sugar-mediated ligand—receptor recognitions via a simple yet highly biospecific interfacial system. *Sci. Rep.* **2013**, *3*, 2293.

(20) Zhang, H.-L.; Wei, X.-L.; Zang, Y.; Cao, J.-Y.; Liu, S.; He, X.-P.; Chen, Q.; Long, Y.-T.; Li, J.; Chen, G.-R.; Chen, K. Fluorogenic Probing of Specific Recognitions between Sugar Ligands and Glycoprotein Receptors on Cancer Cells by an Economic Graphene Nanocomposite. *Adv. Mater.* **2013**, *25*, 4097—4101.

(21) Li, F.; Pei, H.; Wang, L.; Lu, J.; Gao, J.; Jiang, B.; Zhao, X.; Fan, C. Nanomaterial-Based Fluorescent DNA Analysis: A Comparative Study of the Quenching Effects of Graphene Oxide, Carbon Nanotubes, and Gold Nanoparticles. *Adv. Funct. Mater.* **2013**, *23*, 4140—4148.

(22) Trupp, S.; Schweitzer, A.; Mohr, G. J. A fluorescent water-soluble naphthalimide-based receptor for saccharides with highest sensitivity in the physiological pH range. *Org. Biomol. Chem.* **2006**, *4*, 2965—2968.

(23) James, T. D.; Sandanayake, K. R. A. S.; Iguchi, R.; Shinkai, S. Novel Saccharide-Photoinduced Electron Transfer Sensors Based on the Interaction of Boronic Acid and Amine. *J. Am. Chem. Soc.* **1995**, *117*, 8982—8987.

(24) Elfeky, S. A.; Flower, S. E.; Masumoto, N.; D'Hooge, F.; Labarthe, L.; Chen, W.; Len, C.; James, T. D.; Fossey, J. S. Diol Appended Quenchers for Fluorescein Boronic Acid. *Chem.—Asian. J.* **2010**, *5*, 581—588.

(25) Stephenson-Brown, A.; Wang, H.-C.; Iqbal, P.; Preece, J. A.; Long, Y.; Fossey, J. S.; James, T. D.; Mendes, P. M. Glucose selective Surface Plasmon Resonance-based bis-boronic acid sensor. *Analyst* **2013**, *138*, 7140—7145.

(26) Wang, H.-C.; Zhou, H.; Chen, B.; Mendes, P. M.; Fossey, J. S.; James, T. D.; Long, Y.-T. A bis-boronic acid modified electrode for the sensitive and selective determination of glucose concentrations. *Analyst* **2013**, *138*, 7146—7151.

(27) He, X.-P.; Deng, Q.; Cai, L.; Wang, C.-Z.; Zang, Y.; Li, J.; Chen, G.-R.; Tian, H. Fluorogenic Resveratrol-Confined Graphene Oxide for Economic and Rapid Detection of Alzheimer's Disease. *ACS Appl. Mater. Interfaces* **2014**, *6*, 5379—5382.